

Lasers in Manufacturing Conference 2019

## OCT-controlled generation of complex geometries on stainless steel using ultra-short laser pulses

Daniel Holder<sup>a\*</sup>, Steffen Boley<sup>a</sup>, Matthias Buser<sup>a</sup>, Christoph Irion<sup>a</sup>, Rudolf Weber<sup>a</sup>,  
Thomas Graf<sup>a</sup>

*<sup>a</sup>Institut für Strahlwerkzeuge (IFSW), University of Stuttgart, Pfaffenwaldring 43, 70569 Stuttgart, Germany*

---

### Abstract

The generation of complex surface geometries with a defined depth, high contour accuracy, and low roughness in steel with ultra-short pulse laser ablation is still a challenge.

In the present work, optical coherence tomography (OCT) providing high-resolution optical distance measurement of the ablation depth was combined with a Galvanometer-Scanner for fast beam deflection. The actual ablation depth was measured during processing. The online comparison with the target ablation depth was used to select areas that have to be processed in the subsequent pass. This selective material ablation allowed to smooth surface defects caused by inhomogeneous material removal. Furthermore, the selective material ablation was used to generate locally different ablation depths in order to create complex geometries.

As a result, the surface roughness could be significantly reduced compared to the uncontrolled process, and precise ablation of complex geometries on steel was demonstrated.

Keywords: Process Control; Optical Coherence Tomography; Ultra-short Laser Pulses; Controlled and Selective Ablation of Steel; Complex Geometries; Stainless

---

---

\* Corresponding author. Tel.: +49-711-685-69740; fax: +49-711-685-66842.  
E-mail address: daniel.holder@ifsw.uni-stuttgart.de.

## 1. Introduction

Ultra-short pulse laser ablation of complex geometries in steel still represents a challenge when small tolerances and low surface roughness are required. Using optical coherence tomography (OCT) for optical distance measurement is one approach that is already established in laser welding and allows distance measurements with an accuracy in the range of several microns within a measurement range of a few millimeters (Kogel-Hollacher, et al. 2016). The OCT beam and the laser processing beam can be superimposed by means of a dichroitic mirror in order to receive time-resolved information about the drilling progress during laser percussion drilling. This was utilized to control the drilling process of multiple blind holes and thus reduce the standard deviation of the drilling depth of these holes to  $10\text{ }\mu\text{m}$  (Webster, et al. 2010). By combining a Galvanometer-Scanner and a OCT system the measured distance value of the OCT system can be assigned to each position value in the scanning field which enables 3D measurements of the surface topography (Schmitt, et al. 2012). The 3D measurements can be used e.g. to assure the correct sample positioning during a laser decoating process on free-form surfaces (Schaes, et al. 2018).

A controlled and fully automated ablation process is implemented as shown in (Boley, et al. 2017) by comparing actual ablation depth and target depth for each location in the processing area of the scanning field. After each pass the control unit decides where material has to be ablated in the subsequent pass and irradiates areas that have not reached the target depth yet. Controlled ablation of CFRP with a ns-Laser allowed to maintain a low surface roughness of about  $S_a = 10\text{ }\mu\text{m}$  in ablation depths up to 5 mm (Holder, et al. 2018).

In this work an ultra-short pulse laser system in combination with an OCT system is used for controlled and selective material ablation of steel in order to smooth surface defects caused by inhomogeneous material removal and the generation of complex geometries.

## 2. Experimental Setup

The processed material is cold-rolled steel type AISI 304, a stainless steel often used in food industry and mechanical engineering. A schematic representation of the experimental setup is shown in Figure 1. The processing laser beam is guided to a Galvanometer-Scanner before being focused onto the sample surface by means of a F-Theta lens with a focal length of 163 mm resulting in a focal diameter of  $80 \pm 5\text{ }\mu\text{m}$ . A dichroitic mirror is used to superpose the OCT beam to the processing laser beam.

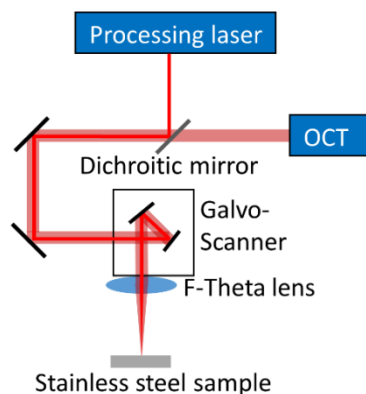


Fig. 1. Schematic representation of the experimental setup using OCT for online measurement of ablated depth.

The processing laser is a home-built mJ-ps-laser system (Negel, et al. 2013) with specifications according to Table 1.

Table 1. Specifications of the processing laser.

Processing laser	Specifications
Wavelength	1030 nm
Pulse duration	8 ps
Max. repetition rate	300 kHz
Max. pulse energy	1.39 mJ

The OCT-based optical distance measurement system is the Precitec CHRcodile 2 with its specifications summarized in Table 2. As the wavelength of the measurement system with  $\lambda = 1080 \pm 20$  nm is close to one of the processing laser with  $\lambda = 1030$  nm both beams are still superposed after deflection and focusing.

Table 2. Specifications of the OCT Precitec CHRcodile 2.

Precitec CHRcodile 2	Specifications
Wavelength	$1080 \pm 20$ nm
Beam quality factor	$< 1.1$
Measurement rate	70 kHz
Measurement range on axis	$< 6$ mm
Measurement accuracy on axis	$\pm 1$ $\mu$ m
Focus diameter	15 $\mu$ m

Controlled ablation is achieved using the PixelMode of the scanner and a subordinated software program whose basic concept is described in (Boley, et al. 2017) and (Holder, et al. 2018). The OCT measurements of the surface topography can be used to analyse the ablated surface after each pass. In order to verify the OCT measurements, the ablated structures were additionally measured by means of a laser-scanning-microscope (LSM) and scanning electron microscope (SEM) after the ablation process. The LSM-measurements were used to calculate the arithmetic average roughness  $R_a$  described by

$$R_a = \frac{1}{L} \int_0^L |z(x)| dx, \quad (1)$$

with  $L$  being the measurement length and  $x$  being the independent variable of the function  $z(x)$ . The mean value of the arithmetic average roughness  $R_a$  from five lines within the measured surface was used to evaluate and compare the different surfaces.

### 3. OCT-controlled ablation for reduction of the surface roughness

In Figure 2 the surface roughness of an OCT-controlled ablation process is compared with the surface roughness resulting from conventional processing. Conventional processing is defined in this work as shown schematically in Figure 1 of (Faas, et al. 2018). Rectangular areas of  $5 \times 1$  mm<sup>2</sup> with were processed with

conventional and controlled ablation up to 560  $\mu\text{m}$  depth in order to investigate the dependence of the resulting roughness on the ablation depth. At the maximum repetition rate of 300 kHz a scanning speed of 5 m/s and hatching distance of 15  $\mu\text{m}$  was used to reach a pulse overlap of about 80 %. The pulse energy was adjusted to achieve a peak fluence of about 1.1 J/cm<sup>2</sup> on the sample surface. The resulting surface roughness for various ablation depths can be seen in Figure 2.

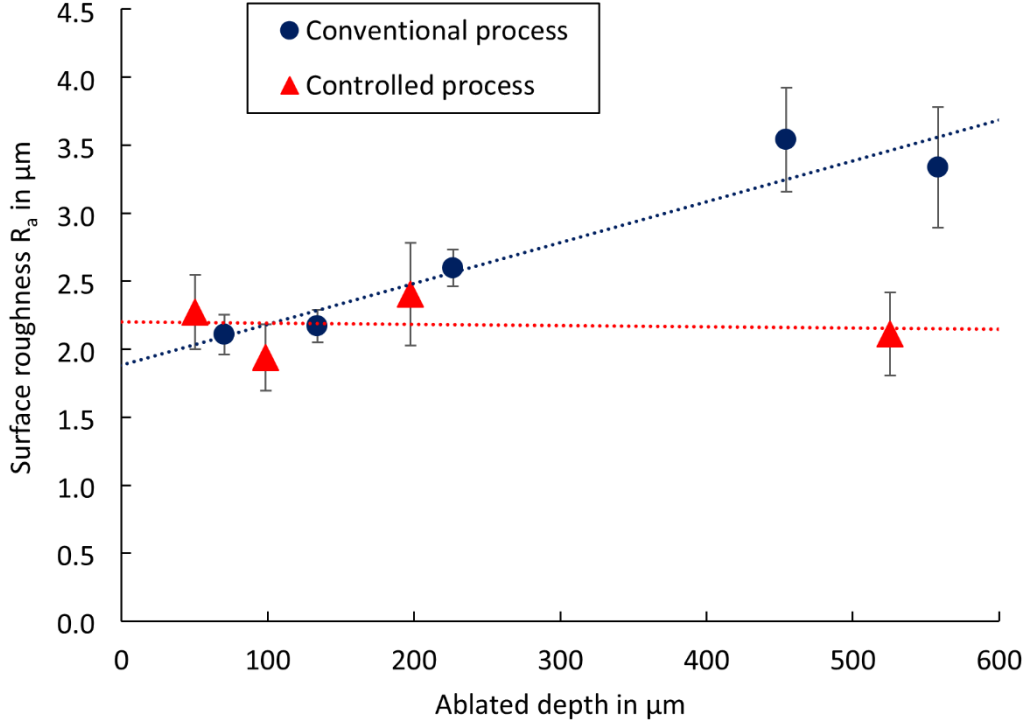


Fig 2. Measured surface roughness  $R_a$  of ablated structures produced with a conventional and a controlled ablation process for various ablation depths.

In the conventional process the roughness increases about linearly with increasing ablation depth, which is probably due to surface defects caused by inhomogeneous material removal. A controlled ablation process yields a constant surface roughness independent of the depth over the investigated range up to 530  $\mu\text{m}$ .

#### 4. OCT-controlled generation of complex geometries

Controlled ablation also allows to produce complex geometries on the original surface. A fabric texture was chosen as a target geometry in order to demonstrate the capability to generate precise structures with very steep slopes. At the maximum repetition rate of 300 kHz a hatching distance of 15  $\mu\text{m}$  was used. In the first step of the ablation process, the scanning speed was adjusted to 2 m/s and the peak fluence to 12.1 J/cm<sup>2</sup> in order to achieve a high ablation rate until about 90% of the target ablation depth was reached. In the second step, the scanning speed was reduced to 1 m/s and the peak fluence to 1.1 J/cm<sup>2</sup> to achieve a smooth surface when the target ablation depth was reached. An OCT- and a SEM-measurement of the resulting surface topography after the controlled ablation process can be seen in Figure 3.

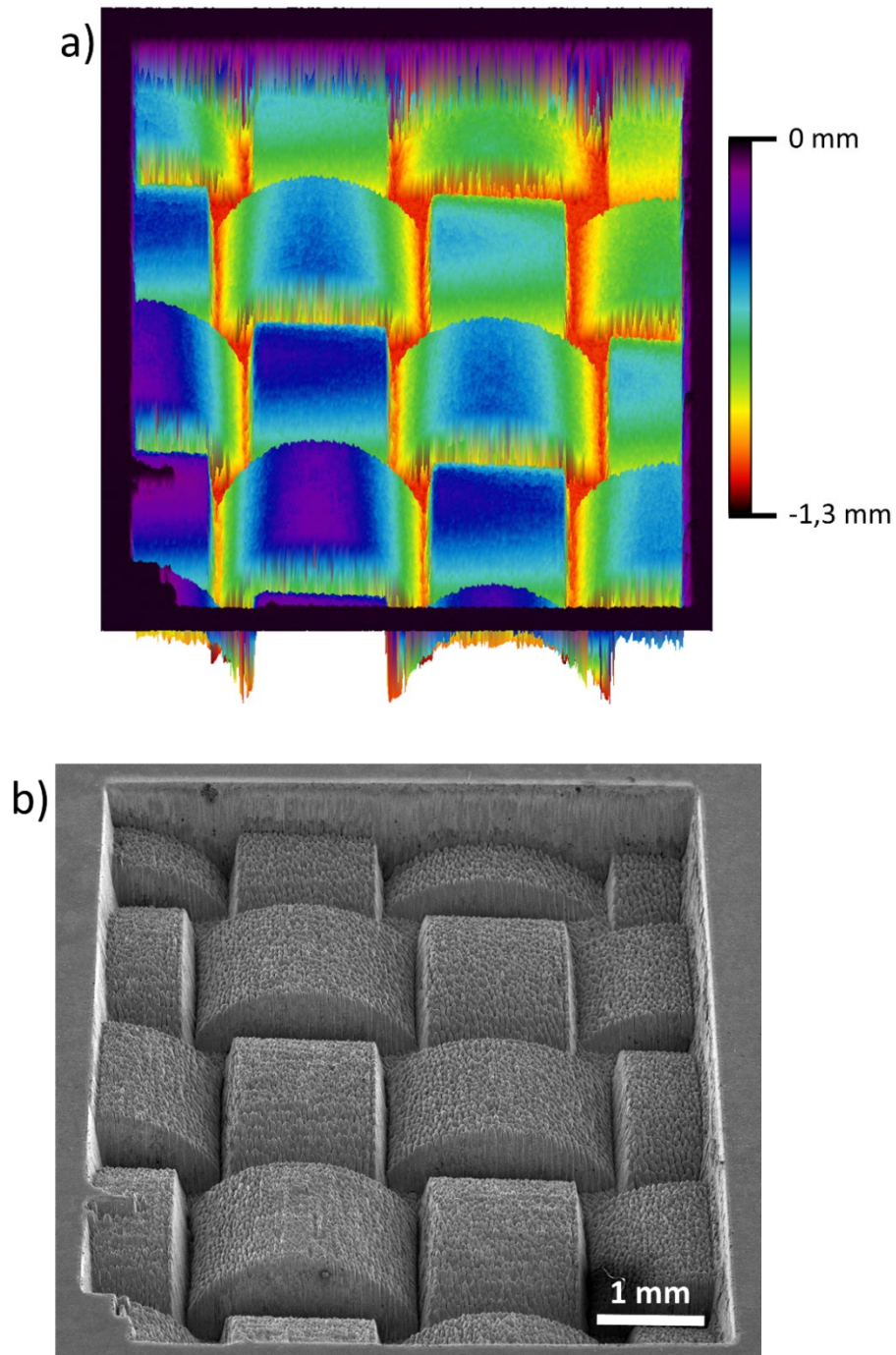


Fig. 3. a) OCT-measurement of surface topography after the controlled ablation process; b) SEM-measurement of the final geometry.

As a result, a complex geometry was generated on the original flat steel surface (Figure 3b) with its features represented in the OCT-measurement (Figure 3a). The process time to generate the geometry in an automated and controlled ablation process was 63 min, including the time for data processing between subsequent passes to select areas that have to be further processed.

## 5. Conclusion

In summary, we have presented an OCT-controlled ablation process for the generation of complex geometries on stainless steel using ultra-short laser pulses. High-resolution optical distance measurement was used to measure the ablation depth during processing. A control unit utilized the measurements in order to select areas that have to be processed in the subsequent pass. The controlled ablation process allowed to smooth surface roughness, yielding a constant surface roughness of less than  $2.5\text{ }\mu\text{m}$  in any ablated depth up to  $530\text{ }\mu\text{m}$ . The controlled and automated laser ablation process was used to demonstrate the complex geometry of a fabric in a steel sample.

## Acknowledgements

This work was supported by the German Federal Ministry of Education and Research BMBF in the frame of the project SCULP<sup>3</sup>T (grant number 13N13931).

## References

- Kogel-Hollacher M., Schoenleber, M., Bautze, T., Strebel, M., Moser, R., 2016. Measurement and Closed-Loop Control of the Penetration Depth in Laser Materials Processing, 9th International Conference on Photonic Technologies LANE, pp. 1-7.
- Webster, P. J. L., Yu, J. X. Z., Leung, B. Y. C., Anderson, M. D., Yang, V. X. D. und Fraser, J. M., 2010. In situ 24 kHz coherent imaging of morphology change in laser percussion drilling, Optics letters, Vol. 35, No. 5, pp. 646-648.
- Schmitt, R., Mallmann, G., Winands K., Pothen M., 2012, Inline process metrology system for the control of laser surface structuring processes, Physics Procedia, No. 39, pp. 814-822.
- Schares, R., Schmitt, S., Emonts, M., Fischer, K., Moser, R., Fruehauf, B., 2018, Improving accuracy of robot-guided 3D laser surface processing by workpiece measurement in a blink, Proceedings of SPIE, High Power Laser Materials Processing: Applications, Diagnostics, and Systems, Vol. 7, pp. 1-12.
- Boley, S., Holder, D., Onuseit, V., Graf, T., Buser, M., Schoenleber, M., 2017, Distance controlled laser ablation of CFRP, Lasers in Manufacturing Conference, pp. 1-9.
- Holder, D., Boley, S., Buser, M., Weber, R., Graf, T., 2018, In-process determination of fiber orientation for layer accurate laser ablation of CFRP, 10th CIRP Conference on Photonic Technologies LANE 2018, Vol. 74, pp. 557-561.
- Negel, J.-P., Voss, A., Abdou Ahmed, M., Bauer, D., Sutter, D., Killi, A., Graf, T., 2013, 1.1 kW average output power from a thin-disk multipass amplifier for ultrashort laser pulses, Optics letters, Vol. 38, No. 24, pp. 5442-5445.
- Faas, S., Bielke, U., Weber, R., Graf, T., 2018, Prediction of the surface structures resulting from heat accumulation during processing with picosecond laser pulses at the average power of 420 W, Applied Physics A, Vol. 124, No. 612, pp. 1-9.
- Targowski, P., Ostrowski, R., Marczak, J., Sylwestrzak, M., Kwiatkowska, E. A., 2009, Picosecond laser ablation system with process control by optical coherence tomography, Proceedings of SPIE, Vol. 7391.